

Colossal Thermoelectric Power Factor in $K_{7/8}RhO_2$

Y. Saeed, N. Singh, and U. Schwingenschgl

PSE Division, KAUST, Thuwal 23955-6900, Kingdom of Saudi Arabia

Abstract

We discuss the thermoelectric and optical properties of layered K_xRhO_2 ($x = 1/2$ and $7/8$) in terms of the electronic structure determined by first principles calculations as well as Boltzmann transport theory. Our optimized lattice constants differ significantly from the experiment, but result in optical and transport properties close to the experiment. The main contribution to the optical spectra are due to intra and inter-band transitions between the Rh $4d$ and O $2p$ states. We find a similar power factor for pristine K_xRhO_2 at low and high cation concentrations. Our transport results of hydrated K_xRhO_2 at room temperature show highest value of the power factor among the hole-type materials. Specially at 100 K, we obtain a value of $3 \times 10^{-3} K^{-1}$ for $K_{7/8}RhO_2$, which is larger than that of $Na_{0.88}CoO_2$ [M. Lee *et al.*, Nat. Mater. 5, 537 (2006)]. In general, the electronic and optical properties of K_xRhO_2 are similar to Na_xCoO_2 with enhanced transport properties in the hydrated phase.

PACS: 71.15.Mb, 71.20.Dg, 72.15.Jf, 78.20-e

Keywords: Layered oxides, Density functional theory, Tra

Layered cobalt oxides are of technological interest because of their transport properties [1–5]. By varying the Na concentration in Na_xCoO_2 the system changes its behaviour from metallic to insulating and becomes superconducting near $x = 0.3$ [3, 4]. Recently, a strong enhancement of the Seebeck coefficient has been reported for $Na_{0.88}CoO_2$ at $T = 80$ K [5], which greatly improves the prospects for thermoelectric applications. The peak value of Seebeck coefficient and the power factor were found to be $200 \mu V/K$ and $1.8 \times 10^{-3} K^{-1}$, respectively, which is among the highest values for hole-type materials below 100 K. This fact has promoted huge interest in the isostructural and isovalent families A_xCoO_2 ($A = K, Rb, Cs$). Angle-resolved photoemission spectroscopy points to similar electronic and optical properties of $K_{1/2}CoO_2$ and $Na_{1/2}CoO_2$, which is also confirmed by band structure calculations [6–9]. The electronic structures of hydrated and unhydrated Na_xCoO_2 is studied by first principles calculations [10].

Analogous compounds with Rh in place of Co are found to be good thermoelectric materials with reduced correlation effects [9, 11–14]. Shibusaki *et al.* [15] have shown that the substitution of Rh ions in $La_{0.8}Sr_{0.2}Co_{1-x}Rh_xO_{3-\delta}$ diminishes the magnetic moment of Co, where the thermopower is enhanced by a factor of 10 at $x = 1/2$ as compared to $x = 0$ and 1. The electronic structure, optical and thermoelectric properties of $K_{0.49}RhO_2$ is investigated by Okazaki *et al.* [16, 17] and found a qualitative similarities in the optical conductivity spectra as compared to Na_xCoO_2 . The experimental Seebeck coefficient of $40 \mu V/K$ (300 K) is reported [17]. The temperature dependence of transport properties is different from those of Na_xCoO_2 , which also suggests that the correlation in the Rh oxides is weaker than in Na_xCoO_2 . An enhancement of the transport properties for an increasing concentration of alkali cations has been reported for other layered oxides as well [18]. Though, various $4d$ systems have been investigated, the electronic structure in general is poorly understood so far [19, 20].

In order to throw light on the inter connection between enhancement of thermoelectric properties and a high cation concentration, first principles calculations of electronic, optical, and thermoelectric prop-

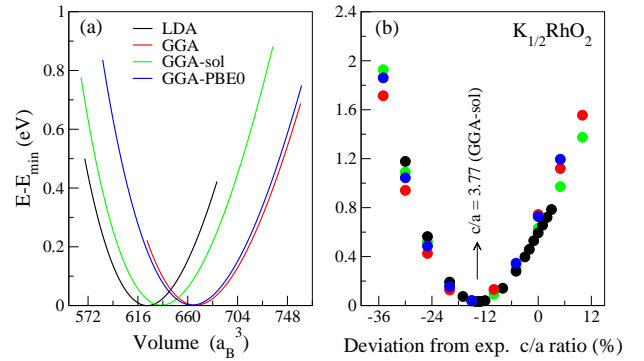


Figure 1: Volume optimization of $K_{1/2}RhO_2$ for different exchange correlation functionals.

erties for K_xRhO_2 ($x = 1/2$ and $7/8$) are performed. The experimental data of optical and transport properties is taken from Refs. [16, 17]. A comparison to Na_xCoO_2 is given in terms of the chemical nature of the Co $3d$ and Rh $4d$ orbitals. The optical transitions are explained by the electronic band structure (BS) and density of states (DOS). The influence of a high cation concentration on power factor is also discussed, which is key for thermoelectric devices.

Our calculations are based on density functional theory (DFT), using the full-potential linearized augmented plane wave approach as implemented in the WIEN2k code [21]. This method has been successfully applied to describe the electronic structure of oxides [22, 23] including the optical spectrum [24]. The transport is calculated by the semiclassical Boltzmann theory within the constant scattering approximation, as implemented in the BoltzTraP code [25]. Various exchange and correlation functionals (local density approximation (LDA), generalized gradient approximation (GGA), GGA-sol, and GGA-PBE0) are used for optimizing the c/a ratio. Since the differences are small, we will discuss in following only GGA-sol results for the electronic, optical and transport properties.

The unit cell is divided into non-overlapping atomic spheres centered at the atomic sites and an interstitial region. The convergence parameter $R_{mt}K_{max}$, where K_{max} is the plane-wave cut-off and R_{mt} is the smallest of all muffin-tin radii controls the size of the basis

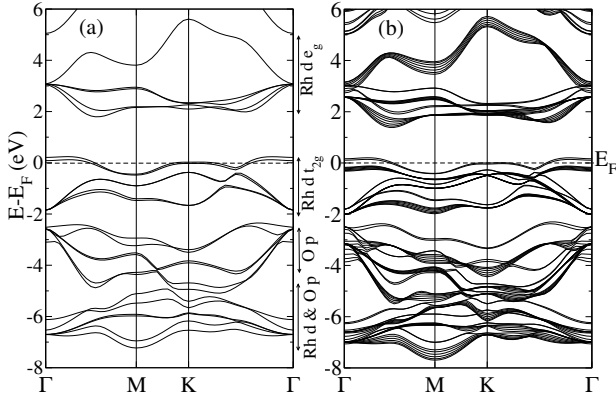


Figure 2: Energy band structures of (a) $K_{1/2}\text{RhO}_2$ and (b) $K_{7/8}\text{RhO}_2$.

set. This convergence parameter is set to 7 together with $G_{max}=24$. We use 66 \mathbf{k} -points in the irreducible wedge of the Brillouin zone for calculating the electronic structure and a dense mesh of 480 \mathbf{k} -points in the optical calculations. For the transport calculations, we use 4592 \mathbf{k} -points. Self-consistency is assumed to be achieved for a total energy convergence of 10^{-5} Ryd.

$K_x\text{RhO}_2$ crystallizes in the $\gamma\text{-Na}_x\text{CoO}_2$ structure (space group $P6_3/mmc$) with the experimental lattice constants $a = 3.0647$ and $c = 13.6$ [26]. The CdI_2 -type RhO_2 layer and the K layer are stacked alternately along the c -axis. The experimental lattice constants of $K_{1/2}\text{RhO}_2$ are used as a starting point of the optimization, obtaining the optimized volume and c/a ratio presented in Fig. 1. Our LDA calculation yields a $\sim 14\%$ reduction of the c/a ratio from 4.44 (experimental) to 3.84 (calculated), which is close to other layered Co/Rh oxides (c/a ratio ~ 3.8). We obtain lattice constants of $a = 3.02$ and $c = 11.63$. The bonding length between Rh and O is reduced from 2.1326 to 2.0395. To confirm the large deviation of the c/a ratio from the experimental structure parameters, we have optimized the structure by more involved exchange correlation functionals (GGA, GGA-sol and PBE0). However, we obtain almost the same results for all functionals. In addition, our optimized lattice parameters are confirmed by calculations of the optical and transport properties, see the discussion below. The calculated Seebeck coefficient is overestimated for the experimental lattice constants, while the optimized lattice constants yield a Seebeck coefficient close to the experiment. The calculated optical conductivity of $K_{1/2}\text{RhO}_2$ (with optimized lattice constants) at zero photon energy is found to be $\sim 2500 \Omega^{-1}\text{cm}^{-1}$, which agrees excellently with the experiment.

The observed difference of the c length between $K_x\text{RhO}_2$ and Na_xCoO_2 could be attributed to the different ionic radii of K and Na. However, our optimized value of c is similar to other isostructural layered oxides such as Sr_xRhO_2 [27, 28], Na_xCoO_2 [7], Li_xNbO_2 [29], and La_xCoO_2 [30]. In addition, LiRhO_2 , NaRhO_2 , and KRhO_2 layered oxides can form a hydrate (water intercalated) phase [19] with an

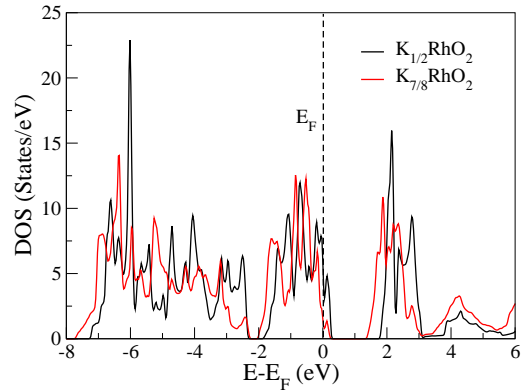


Figure 3: DOS obtained for $K_{1/2}\text{RhO}_2$ and $K_{7/8}\text{RhO}_2$.

increased c length [31]. Takada *et al.* [4] showed that Na_xCoO_2 can be readily hydrated to form $\text{Na}_x\text{CoO}_2 \cdot y\text{H}_2\text{O}$, maintaining the CoO_2 layers, but with a considerably expanded c axis, to accommodate the intercalated water. In the following, the optimized lattice constants are used, unless stated otherwise.

In Figs. 2 (a) and (b) the calculated electronic BSs of $K_{1/2}\text{RhO}_2$ and $K_{7/8}\text{RhO}_2$ is presented. The BS of $K_{1/2}\text{RhO}_2$ is similar to isostructural and isovalent $\text{Na}_{1/2}\text{CoO}_2$, except for a slightly larger pseudogap. Moreover, the strongly dispersive bands and high hole concentration in $K_{7/8}\text{RhO}_2$ give rise to a high thermoelectricity. The calculated DOS (Fig. 3) shows a crystal field splitting experienced by the Rh^{4+} ions (splitting into e_g and t_{2g} states) is similar to the Co^{3+} case, but with a larger bandwidth. The bandwidth of the t_{2g} state is 1.52 eV for Rh^{4+} and 1.46 eV for Co^{3+} in the case of $K_{1/2}\text{CoO}_2$ (not shown here). A similar increment is also observed for the e_g states, in agreement with the experiment [16]. In addition, a weak hybridization is observed between the Rh 4d and O 2p states at/below the Fermi level. The O p states lie deep in the valence band (below -2 eV) as compared to $\text{Na}_{0.50}\text{CoO}_2$. The DOS of $K_{7/8}\text{RhO}_2$ shows increased bandwidths of the e_g and t_{2g} states, which reflects a reduction of the electronic correlation effects in $K_{7/8}\text{RhO}_2$ as compared to Na_xCoO_2 .

The optical properties of $K_x\text{RhO}_2$ ($x = 1/2$ and $7/8$) are studied and presented in Figs. 4(a) and 4(b). The experimental results are taken from Ref. [17]. The obtained reflectivities of $K_{1/2}\text{RhO}_2$ and $K_{7/8}\text{RhO}_2$ (Fig. 4(a)) are similar to each other with a maximum value of $\sim 90\%$ near 0 eV. A Drude-like edge in the optical reflectivity of $K_{1/2}\text{RhO}_2$ is found at ~ 1 eV (experiment: 1.2 eV), while for $K_{7/8}\text{RhO}_2$ this edge appears at ~ 0.5 eV. At zero photon energy, the calculated optical conductivity of $\sigma \sim 2500 \Omega^{-1}\text{cm}^{-1}$ for $K_{1/2}\text{RhO}_2$ is obtained in excellent agreement with the experiment (blue and black dots in fig. 4(b)). Three well defined peaks are observed: (i) near 1 eV due to the intra-band transition of Rh ($t_{2g}-t_{2g}$), (ii) at ~ 3 eV due to the inter-band transition of Rh 4d ($t_{2g}-e_g$), and (iii) around 5.5 eV due to the inter-band transition from the O 2p to the Rh 4d e_g states. These peaks are also present in the experiment [16] as well as for $\text{Na}_{1/2}\text{CoO}_2$ (0.5 eV, 1.6 eV, and 3 eV, respectively) [6], which again reflects the similarity between these

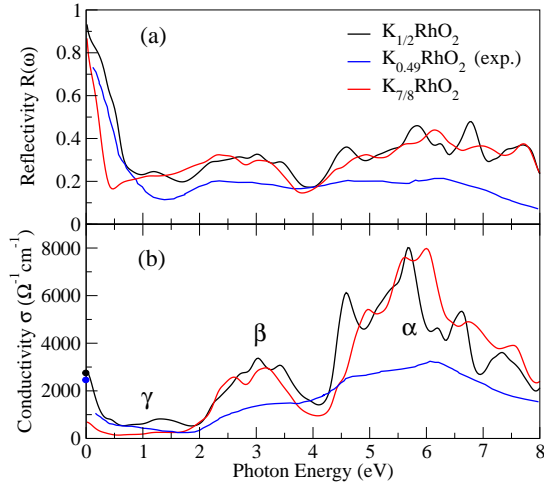


Figure 4: Optical reflectivity and conductivity of $K_{1/2}\text{RhO}_2$ and $K_{7/8}\text{RhO}_2$ along with experimental data [16]. Blue and black dots represent the calculated and experimental values at zero photon energy.

isostructural and isovalent compounds.

In the following, we will address both the experimental crystal structure (hydrated) and optimized structure of $K_x\text{RhO}_2$. We have calculated the Seebeck coefficient (S), thermal conductivity (κ), and power factor (Z). The results are plotted in Figs. 5(a), (b), and (c) as a function of the temperature from 0 to 700 K, and compared with the experimental Z of $\text{Na}_{0.88}\text{CoO}_2$ [5]. Fig. 5(a) shows that the calculated S of pristine $K_x\text{RhO}_2$ is $\sim 50 \mu\text{V}/\text{K}$ at 300 K, in agreement with the experiment ($40 \mu\text{V}/\text{K}$) [17]. The calculated S values of hydrated $K_{1/2}\text{RhO}_2$ and $K_{7/8}\text{RhO}_2$ are strongly enhanced, amounting to $\sim 100 \mu\text{V}/\text{K}$ and $\sim 140 \mu\text{V}/\text{K}$, respectively. The calculated S of pristine $K_x\text{RhO}_2$ hardly depends on the K concentration upto 300 K, while for higher temperature for $K_{7/8}\text{RhO}_2$ increases stronger to reach a value of $80 \mu\text{V}/\text{K}$ at 700 K. In contrast to this behavior, the calculated S of hydrated $K_x\text{RhO}_2$ remains almost constant above 300 K. According to Fig. 5(b) the thermal conductivity is similar for the hydrated compounds and for pristine $K_{7/8}\text{RhO}_2$, while its much enhanced for pristine $K_{1/2}\text{RhO}_2$.

In Fig. 5(c), the calculated power factor Z of pristine and hydrated $K_x\text{RhO}_2$ along with experimental data for $\text{Na}_{0.88}\text{CoO}_2$ [5] is presented. Upto 25 K, power factor of hydrated $K_{7/8}\text{RhO}_2$ behaves similar to the experimental curve, but approaches a value of $3 \times 10^{-3} \text{ K}^{-1}$ at 100 K, which is much higher than that of other hole-type materials (like $\text{Na}_{0.88}\text{CoO}_2$ $Z = 1.8 \times 10^{-3} \text{ K}^{-1}$ at 80 K) in this temperature range. Even at room temperature (300 K), the calculated Z value for hydrated $K_x\text{RhO}_2$ is much higher than $\text{Na}_{0.88}\text{CoO}_2$, while for pristine $K_x\text{RhO}_2$ is just slightly greater. The large power factor in hydrated $K_x\text{RhO}_2$ results from a decrease of the thermal conductivity, increase in the electrical conductivity as reported for the hydrated phase of NaRhO_2 (Fig. 2 of Ref. [31]), and larger S as compared to that of pristine $K_x\text{RhO}_2$. Therefore, the transport properties of hydrated $K_x\text{RhO}_2$ are highly promising for technological

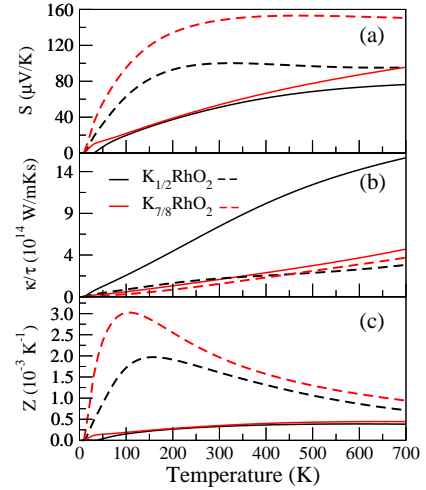


Figure 5: Calculated thermoelectric properties of pristine (solid line) and hydrated (dashed line) $K_x\text{RhO}_2$. Experimental data from Ref. [5] is included.

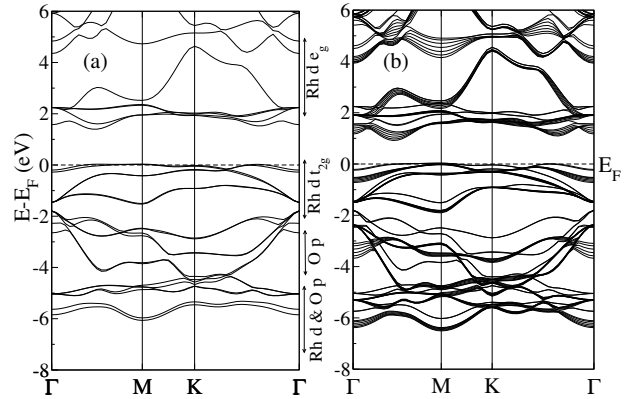


Figure 6: $K\text{RhO}_2$ -hydrated

applications.

In conclusion, the electronic, optical, and transport properties of layered $K_x\text{RhO}_2$ ($x = 1/2$ and $7/8$) are calculated, and compared to the isostructural and isovalent compound Na_xCoO_2 . Our optimized structure of $K_{1/2}\text{RhO}_2$ shows a huge deviation in the c/a ratio from the experiment but gives a good agreement for the optical and transport properties. The large deviations, also in comparison the other related compounds, indicate that the experimental structure has been determined for the hydrated phase of $K_x\text{RhO}_2$. The $\text{Rh}^{4+}4d e_g$ and t_{2g} states of $K_{1/2}\text{RhO}_2$ are broader than the respective Co^{3+} states in Na_xCoO_2 , which confirms previous reports. The calculated Seebeck coefficient of pristine $K_x\text{RhO}_2$ ($x = 1/2$ and $7/8$) is $S \sim 50 \mu\text{V}/\text{K}$ at room temperature, which is close to the experimental value of $S = 40 \mu\text{V}/\text{K}$. Our calculations also show large values of S and Z for hydrated $K_x\text{RhO}_2$ in whole temperature range from 0 to 700 K. At around 100 K, the calculated Z of hydrated $K_{7/8}\text{RhO}_2$ is $3 \times 10^{-3} \text{ K}^{-1}$, which is the highest value in any hole-type material at this temperature. At room temperature, the calculated Z value of pristine $K_x\text{RhO}_2$ is $\sim 0.4 \times 10^{-3} \text{ K}^{-1}$, which is also slightly greater than that of $\text{Na}_{0.88}\text{CoO}_2$.

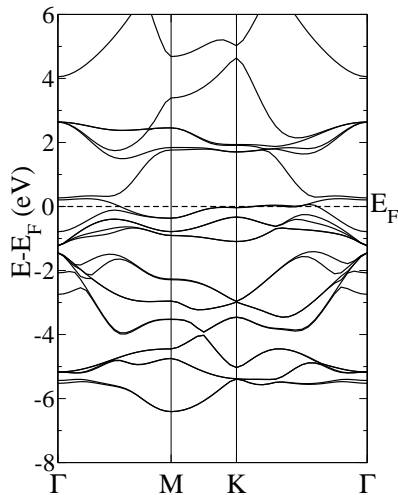


Figure 7: Band Na₅₀CoO₂ c15.6A

Therefore, our results suggest that hydration can be used to elongate the structure and inducing the doping by the formation of hydronium ions, results strong enhancement of thermoelectric properties of this class of layered oxides.

-
- [1] I. Terasaki, Y. Sasago, and K. Uchinokura, *Phys. Rev. B* 56, R12685 (1997).
- [2] T. Motohashi, R. Ueda, E. Naujalis, T. Tojo, I. Terasaki, T. Atake, M. Karppinen, and H. Yamauchi, *Phys. Rev. B* 67, 064406 (2003).
- [3] M. L. Foo, Y. Wang, S. Watauchi, H. W. Zandbergen, T. He, R. J. Cava, and N. P. Ong, *Phys. Rev. Lett.* 92, 247001 (2004).
- [4] K. Takada, H. Sakurai, E. Takayama-Muromachi, F. Izumi, R. A. Dilanian, and T. Sasaki, *Nature (London)* 422, 53 (2003).
- [5] M. Lee, L. Viciu, L. Li, Y. Wang, M. L. Foo, S. Watauchi, R. A. Pascal, R. J. Cava, and N. P. Ong, *Nat. Mater.* 5, 537 (2006).
- [6] M. D. Johannes, I. I. Mazin, and D. J. Singh, *Phys. Rev. B* 71, 205103 (2005).
- [7] J. Sugiyama, H. Nozaki, Y. Ikedo, K. Mukai, J. H. Brewer, E. J. Ansaldo, G. D. Morris, D. Andreica, A. Amato, T. Fujii, and A. Asamitsu, *Phys. Rev. Lett.* 96, 037206 (2006).
- [8] J. Sugiyama, Y. Ikedo, P. L. Russo, H. Nozaki, K. Mukai, D. Andreica, A. Amato, M. Blangero, and C. Delmas, *Phys. Rev. B* 76, 104412 (2007).
- [9] K. W. Lee and W. E. Pickett, *Phys. Rev. B* 76, 134510 (2007).
- [10] M. D. Johannes and D. J. Singh, *Phys. Rev. B* 70, 014507 (2004).
- [11] Y. Klein, S. Hébert, D. Pelloquin, V. Hardy, and A. Maignan, *Phys. Rev. B* 73, 165121 (2006).
- [12] S. Shibusaki, W. Kobayashi, and I. Terasaki, *Phys. Rev. B* 74, 235110 (2006).
- [13] W. Kobayashi, S. Hébert, D. Pelloquin, O. Perez, and A. Maignan, *Phys. Rev. B* 76, 245102 (2007).
- [14] W. Koshibae, K. Tsutsui, and S. Maekawa, *Phys. Rev. B* 62, 6869 (2000).
- [15] S. Shibusaki, I. Terasaki, E. Nishibori, H. Sawa, J. Lybeck, H. Yamauchi, and M. Karppinen, *Phys. Rev. B* 83, 094405 (2011).
- [16] R. Okazaki, Y. Nishina, Y. Yasui, S. Shibusaki, and I. Terasaki, *Phys. Rev. B* 84, 075110 (2011).
- [17] S. Shibusaki, T. Nakano, I. Terasaki, K. Yubuta, and T. Kajitani, *J. Phys. Condens. Matter* 22, 115603 (2010).
- [18] T. Motohashi, Y. Sugimoto, Y. Masubuchi, T. Sasagawa, W. Koshibae, T. Tohyama, H. Yamauchi, and S. Kikkawa, *Phys. Rev. B* 83, 195128 (2011).
- [19] A. Mendiboure, H. Eickenbusch, and R. Schollhorn, *J. Solid State Chem.* 71, 19 (1987).
- [20] A. Varela, M. Parras, and J. M. González-Calbet, *Eur. J. Inorg. Chem.* 2005, 4410 (2005).
- [21] P. Blaha, K. Schwarz, G. Madsen, D. Kvasnicka, and J. Luitz, WIEN2k, An Augmented Plane Wave + Local Orbitals Program for Calculating Crystal Properties (TU Vienna, Vienna, 2001).
- [22] U. Schwingenschlögl and C. Schuster, *Phys. Rev. Lett.* 99, 237206 (2007); *EPL* 79, 27003 (2007).
- [23] U. Schwingenschlögl, C. Schuster, and R. Frésard, *EPL* 88, 67008 (2009); *EPL* 81, 27002 (2008).
- [24] N. Singh and U. Schwingenschlögl, *Chem. Phys. Lett.* 508, 29 (2011); N. Singh, S. M. Saini, T. Nautiyal, and S. Auluck, *J. Appl. Phys.* 100, 083525 (2006).
- [25] G. K. H. Madsen, K. Schwarz, P. Blaha, and D. J. Singh, *Phys. Rev. B* 68, 125212 (2003).
- [26] K. Yubuta, S. Shibusaki, I. Terasaki, and T. Kajitani, *Philos. Mag.* 89, 2813 (2009).
- [27] A. L. Hector, W. Levason, and M. T. Weller, *Eur. J. Solid State Inorg. Chem.* 35, 679 (1998).
- [28] Y. Okamoto, M. Nohara, F. Akai, and H. Takagi, *J. Phys. Soc. Jap.* 75, 023704 (2006).
- [29] K.-W. Lee, J. Kuneš, R. T. Scalettar, and W. E. Pickett, *Phys. Rev. B* 76, 144513 (2007).
- [30] K. Knížek, J. Hejtmánek, M. Maryško, E. Šantavá, Z. Jiráček, J. Buršík, K. Kirakci, P. Beran, *J. Solid State Chem.* 184, 2231 (2011).
- [31] S. Park, K. Kang, W. Si, W. S. Yoon, Y. Lee, A. R. Moodenbaugh, L. H. Lewis, and T. Vogt, *Solid State Commun.* 135, 51 (2005).